PROGRESS IN MECHANICALLY SHUTTERED TIME-RESOLVED PHOTOLUMINESCENCE IMAGING OF SILICON WAFERS

D. Kiliani, G. Micard, A. Herguth, G. Hahn
University of Konstanz, Department of Physics, 78457 Konstanz, Germany

ABSTRACT: Recently two approaches to extend the photoluminescence imaging (PLI) technique by evaluating the dynamic properties of the sample have been presented. Time-resolved photoluminescence measurements may provide calibration-free maps of the effective minority charge carrier lifetime in silicon wafers. Due to the transient measurement they minimize errors due to lateral inhomogeneities in setup or sample, which would usually contribute linearly to steady-state PLI measurements. In this work, we will focus on mechanically shuttered time-resolved photoluminescence imaging (TR-PLI), as it provides a high measurement range down to 5 µs at low hardware costs.
Keywords: Photoluminescence, Lifetime, Silicon

1 INTRODUCTION

Methods to measure the effective lifetime of excess charge carriers in silicon can generally be divided into two different approaches: steady-state measurements, where the absolute value of a quantity corresponding to the excess charge carrier density Δn is determined under steady-state excitation, and transient measurements, where the dynamic response of such a quantity to fast changes in excitation is determined. Steady-state methods like quasi-steady-state photoconductance (QSSPC) have the advantage that no fast excitation and measurement are required. However, these methods require some sort of calibration to link the measured value to an effective lifetime.

Until recently, camera-based photoluminescence imaging (PLI) was only used as a steady-state technique for lifetime measurements [1], usually in combination with other methods for calibration [2,3]. Last year, two different approaches for transient PLI were presented:

Herlufsen et al. [4] used a fast camera with an InGaAs CMOS sensor to obtain PL images with short exposure times during the periodic illumination of the sample. Many of those images are averaged by the software and used to calculate a map of the effective carrier lifetime. A theoretical measurement range down to 30 µs was reported for the setup.

The method presented by our group [5] also applied a periodic illumination to the sample. The resulting PL emission was modulated by a rotating mechanical shutter/chopper wheel between camera and sample and integrated during a relatively long exposure of the recording silicon CCD camera. Apart from the lower cost of silicon cameras, this has the benefit of recording the camera readout noise only once. However, due to size and speed constraints on the chopper wheel, only effective lifetimes above ~300 µs could be reliably measured with this setup.

In the last months, the time resolution could be significantly improved by some relatively small changes in the measurement setup. The new measurement setup and procedure will be described in this work, with a focus on determining the lower limit of resolvable lifetimes with the current equipment. As the time-resolution of this technique is mainly determined by the chopper frequency, there is no upper limit of the measurement range, as the chopper wheel can be rotated arbitrarily slow.

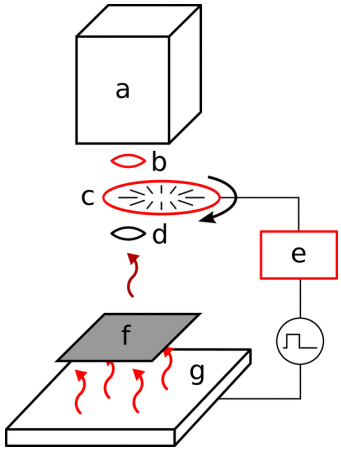

Figure 1: Schematic layout of the measurement setup. A Si-wafer (f) is illuminated by the LED panel (g) and emits PL light. The chopper wheel (c) is positioned at the intermediate image plane between the two lenses (b and d) and has a large number of slits. The CCD camera (a) records the chopped PL signal.

2 MEASUREMENT SETUP

The measurement setup was fundamentally improved since the first publication of this method [5]. The schematic layout of the current measurement setup for time-resolved photoluminescence imaging (TR-PLI) is shown in Fig. 1. A silicon CCD camera (a) was used to record the photoluminescence light through a rotating chopper wheel. The chopper wheel has sectoral slits with a mark to space ratio of 1:1. Two objective lenses (b and d) are used to create an intermediate image plane between camera and sample. The chopper wheel is rotated in this intermediate image plane, so both the sample and the chopper wheel are in focus. The blurring effect of the earlier setup [5], which stems from the unfocused chopper wheel, is therefore eliminated (see Fig. 2 for comparison). This has several positive aspects:

- The aperture of the objective lenses can be chosen as large as necessary for a high sensitivity of the system at low luminescence intensities. No compromise between low blurring and high sensitivity has to be made.
- Because the luminescence light is focused when passing the chopper wheel, the minimal slit width of the chopper wheel is not limited by the lens aperture. The number of slits in the chopper wheel can therefore be increased substantially, leading to much higher obtainable chopper frequencies despite the same

angular velocity. This improves the time-resolution of the measurement, which depends linearly on the chopper frequency.

- The evaluation procedure is simplified, as the blurring function does not have to be modeled. The evaluation is described in detail in the following section.

With these changes to the chopper wheel location and a more powerful motor for rotation, chopper frequencies up to ~12 kHz are currently possible.

The sample (f) is placed beneath the camera on an LED panel (g) and illuminated homogeneously from below. The LED panel emits an adjustable photon flux E of up to 2.5×10^{17} $cm^{-2}s^{-1}$ – about 1 sun equivalent – at 630 nm and can be switched on and off by an excitation control box (e). This excitation controller features a software-based phase-locked loop (PLL) to precisely synchronize the LED panel to the chopper wheel.

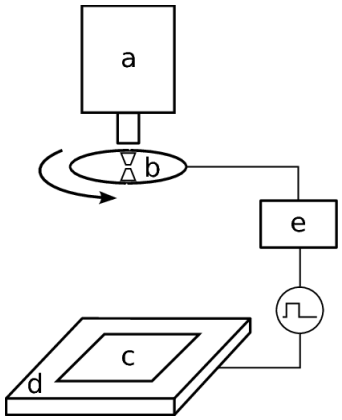

Figure 2: Layout of the previous measurement setup. The chopper wheel (b) is placed in front of the objective lens and therefore not in focus.

The sample is therefore periodically illuminated for 50% of the period length T, while the chopper wheel slits always uncover the light path of a pixel at a defined phase of this excitation cycle. This allows for a pump-probe measurement of the PL emission at each point of the sample with a much higher time-resolution than the camera itself could obtain. By changing the rotation speed of the chopper wheel, excitation periods between 80 µs and 10 ms are selectable to measure samples of different effective lifetime with optimal time-resolution. Best results were obtained with excitation periods of about 2 to 5 times the maximum effective lifetime in the sample.

It has to be noted that the pulsed illumination of the LED panel also has finite switching times, which could affect the measurement for low lifetime samples. However, recordings of the LED response with a fast Si photo-diode showed rise/fall times < 1 µs (10 to 90%). This effect was therefore neglected for the measurements shown in this work.

The actual measurement consists of several PL images taken at different phase delays φ between chopper wheel and LED excitation (see Fig. 3). The effective lifetime for each pixel is then calculated from this set of PL images.

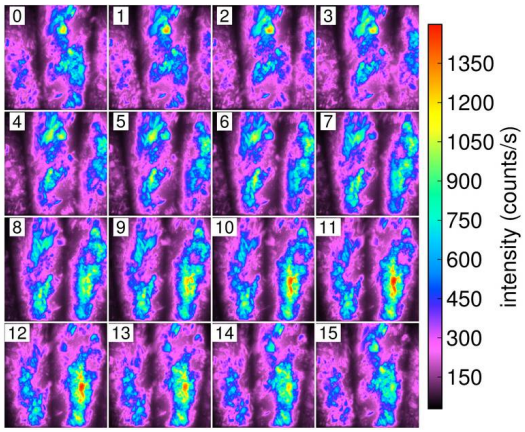

Figure 3: The 16 PL images of a TR-PLI measurement. The images were recorded with 5 s exposure time and an increasing phase delay $\varphi_n = 2\pi\, n/16$.

3 EVALUATION

To calculate effective lifetime values from the set of recorded PL images, a theoretical model for the camera signal I_n of image n was developed.

The LED illumination is switched on at t = 0 and switched off at t = T/2, where T is the period of the excitation cycle. Assuming negligible switching times, we obtain the time-dependent generation rate

$$G(t) = \begin{cases} E(1-R)/w & \text{for } t < T/2, \\ 0 & \text{for } t > T/2 \end{cases}$$

as a rectangular function, where E is the incident photon flux depending on the LED intensity, R is the reflectivity of the sample and w is the thickness of the sample. The use of this thickness-averaged G(t) is a simplification of the actual depth-dependent quantity. Numerical simulations of the transient PL signal showed no relevant influence of this simplification on the shape of the transient under the conditions found in actual Si wafers. In order to keep the model simple, the use of averaged values instead of depth-dependent quantities was therefore deemed acceptable in this case.

The generation rate is the inhomogeneity in the differential equation for the excess carrier density Δn:

$$\frac{d\Delta n}{dt} + \frac{\Delta n}{\tau_{\text{eff}}} = G(t).$$

The general solution to this equation for a constant τ_{eff} is an exponential decay. When taking into account the inhomogeneity G(t) and the periodic boundary condition Δn(0) = Δn(T), we obtain

$$\Delta n(t) = \begin{cases} \Delta n_0 \left(1 - f \exp(-\frac{t}{\tau_{\text{eff}}})\right) & \text{for } t < T/2, \\ \Delta n_0 \left(f \exp(-\frac{t-T/2}{\tau_{\text{eff}}})\right) & \text{for } t > T/2 \end{cases}$$

where Δn_0 is the excess carrier density under steady-state illumination and f is an amplitude factor resulting from the periodic boundary condition:

$$f = \frac{1}{1 + \exp(-T/2\tau_{\text{eff}})}.$$

This condition is valid in the long-term steady-state when the sample has been periodically illuminated for much longer than τ_{eff} and the integral values of carrier

generation and recombination over an excitation cycle are equal.

The excess carrier density determines the amount of radiative recombination

$$\Phi(\Delta n) = B\,\Delta n(N + \Delta n),$$

where N is the doping concentration of the wafer and B is the (constant) coefficient of radiative recombination. Convolving this time-dependent PL intensity Φ(t) with the transmission function H(t) of the chopper wheel yields the integral intensity seen by the camera

$$I_{n,i} = \int_0^T \Phi_i(t)H(t)dt = \int_{t_1(n,i)}^{t_2(n,i)} \Phi_i(t)dt.$$

Due to the rectangular shape of the chopper transmission function H(t), the convolution integral can be written as a simple integral from t_1 to t_2, where $t_1 = (\varphi_n + \theta_i)T/2\pi$ and $t_2 = t_1 + T/2$. The phase offset is split into a global part φ_n depending on the image number n and a local part θ_i. The index i denotes the lateral position on the wafer. θ_i depends on this lateral position, as the chopper wheel phase as seen by each pixel i is different, depending on the chopper rotation and the size of the intermediate image.

Using this model, the acquired camera values $I_{n,i}$ can be fitted to obtain $\tau_{eff,i}$ for each pixel of the sample. Note that the local phase offset θ_i should not be fitted individually but determined globally for all pixels from the geometric properties of the chopper wheel.

4 RESULTS

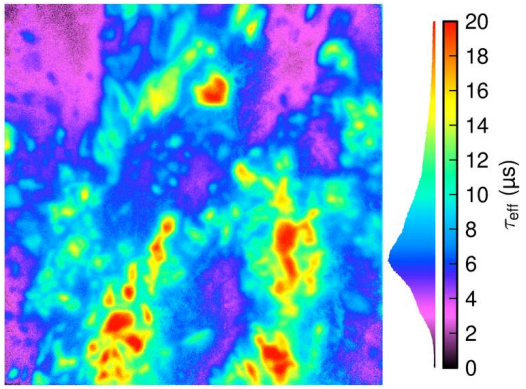

Figure 4: TR-PLI lifetime map of a 5 cm wide mc-Si wafer with SiN_x-passivation of both surfaces. The illuminating photon flux was 2.5×10^{17} cm^{-2}s^{-1} and the chopper frequency 10 kHz.

To determine the lower limit of resolvable effective carrier lifetime with the new setup, a multicrystalline silicon wafer with a SiN_x-passivation of both surfaces and no further gettering or passivation steps was prepared. An area of 5×5 cm^2 was measured with TR-PLI, steady-state PLI and microwave-detected photoconductance decay (MW-PCD). The TR-PLI measurement consists of the 16 PL images shown in Fig. 3, which were taken at E = 2.5×10^{17} cm^{-2}s^{-1} and an exposure time of 5 s each. As can be seen in the following figures, the TR-PLI lifetime map (Figure 4) matches very well to the steady-state PL intensity (Figure 5). Only for very low τ_{eff}, the TR-PLI image shows noticeably less contrast than PLI. This is caused by the scattering of PL radiation and the diffusion of charge carriers from adjacent areas of higher effective lifetime, leading to the detection of a higher transient lifetime compared to the steady-state measurement [3]. Similar effects have been reported earlier for dynamic measurements of free carrier absorption (CDI/ILM) [6]. A possible way to deal with this effect is to use the high lifetime areas of the TR-PLI map for a calibration of the steady-state PL image. However, this again assumes lateral homogeneity of the relation between PL intensity and effective lifetime.

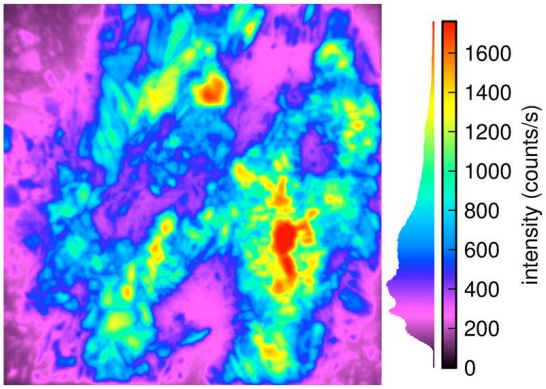

Figure 5: Steady-state PL image of the wafer shown in Fig. 4.

The MW-PCD measurement (Fig. 6) also shows a good qualitative and quantitative agreement with the TR-PLI lifetime map. A relatively small time window was chosen for MW-PCD to obtain a good resolution for low lifetimes, leading to some unresolved (black) pixels with high τ_{eff}. The absolute values of the MW-PCD measurement are generally a little bit higher than the TR-PLI lifetimes. This may be caused by different injection levels Δn, as the carrier density usually has an influence on the effective excess carrier lifetime. The maximum Δn for the TR-PLI measurement can be estimated to ~2×10^{14} cm^{-3} by the product of generation rate and τ_{eff}. For MW-PCD, the injection level unfortunately could not be estimated reliably.

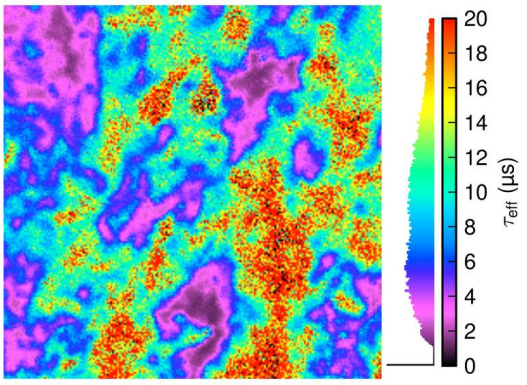

Figure 6: MW-PCD measurement of the sample shown in Fig. 4.

A similar multicrystalline wafer was used for a comparison of quasi-steady-state photoconductance (QSSPC) with the average lifetime of a TR-PLI measurement. The result is shown in Fig. 7, where τ_{eff} is plotted against the injection level Δn. The averaged TR-PLI lifetime of 15.2 µs is shown by the circle at an averaged injection level of about 2×10^{14} cm^{-3}. As the

intensity of the LED panel is limited to about 1 sun equivalent, higher values of Δn could not be reached. On the other hand, QSSPC is affected by charge carrier trapping at low injection [7] and the difference between the two methods may well be caused by the resulting overestimation of τ_{eff}.

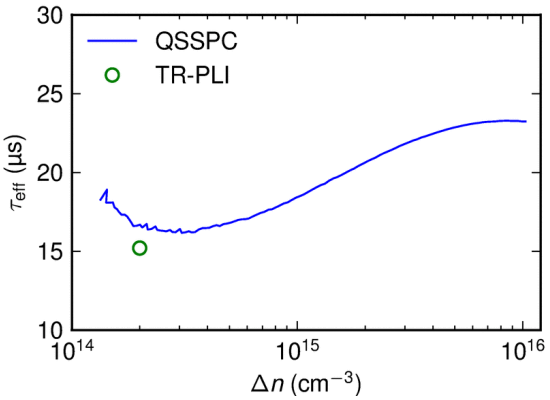

Figure 7: Comparison of QSSPC lifetime measurement and averaged TR-PLI lifetime map for a mc-Si wafer.

5 CONCLUSION

The new setup using a chopper wheel in an intermediate image plane can significantly improve the time-resolution of the mechanically shuttered TR-PLI technique. Effective minority charge carrier lifetimes down to 5 µs could reliably be measured with a silicon CCD camera and ~80 s of total exposure time. As the method determines the transient carrier lifetime, no external calibration is required. Quantitative comparison to MW-PCD and QSSPC measurements shows good agreement, although interference of adjacent areas may lead to a loss of contrast in wafers with strong lateral variations of τ_{eff}. For such samples it may be applicable to use a steady-state PLI measurement calibrated with TR-PLI.
Mechanically shuttered TR-PLI therefore offers a high measurement range at comparably low equipment costs, as the technique imposes no constraints on the camera speed.

6 ACKNOWLEDGEMENTS

The financial support of the German BMU project FKZ 325033 is gratefully acknowledged. The content of this publication is the responsibility of the authors.

7 REFERENCES

[1] T. Trupke, R.A. Bardos, M.C. Schubert, W. Warta, Appl. Phys. Lett. **89**, 044107 (2006).

[2] S. Herlufsen, J. Schmidt, D. Hinken, K. Bothe, R. Brendel, Phys. Stat. Sol. (RRL) **2**, 245-247 (2008).

[3] J.A. Giesecke, M.C. Schubert, B. Michl, F. Schindler, W. Warta, Sol. En. Mat. and Solar Cells **95**, 1011-1018 (2010).

[4] S. Herlufsen, K. Ramspeck, D. Hinken, A. Schmidt, J. Müller, K. Bothe, J. Schmidt, R. Brendel, Phys. Stat. Sol. (RRL) **5**, 25-27 (2011).

[5] D. Kiliani, G. Micard, B. Raabe, G. Hahn, Proc. 25th EU PVSEC, Valencia 2010, pp. 1363-1366.

[6] K. Ramspeck, K. Bothe, J. Schmidt, R. Brendel, J. Appl. Phys. **106**, 114506 (2009).

[7] R.A. Sinton, A. Cuevas, M. Stuckings, Proc. 25th IEEE PVSC, Waikoloa 2006, pp. 457-460.